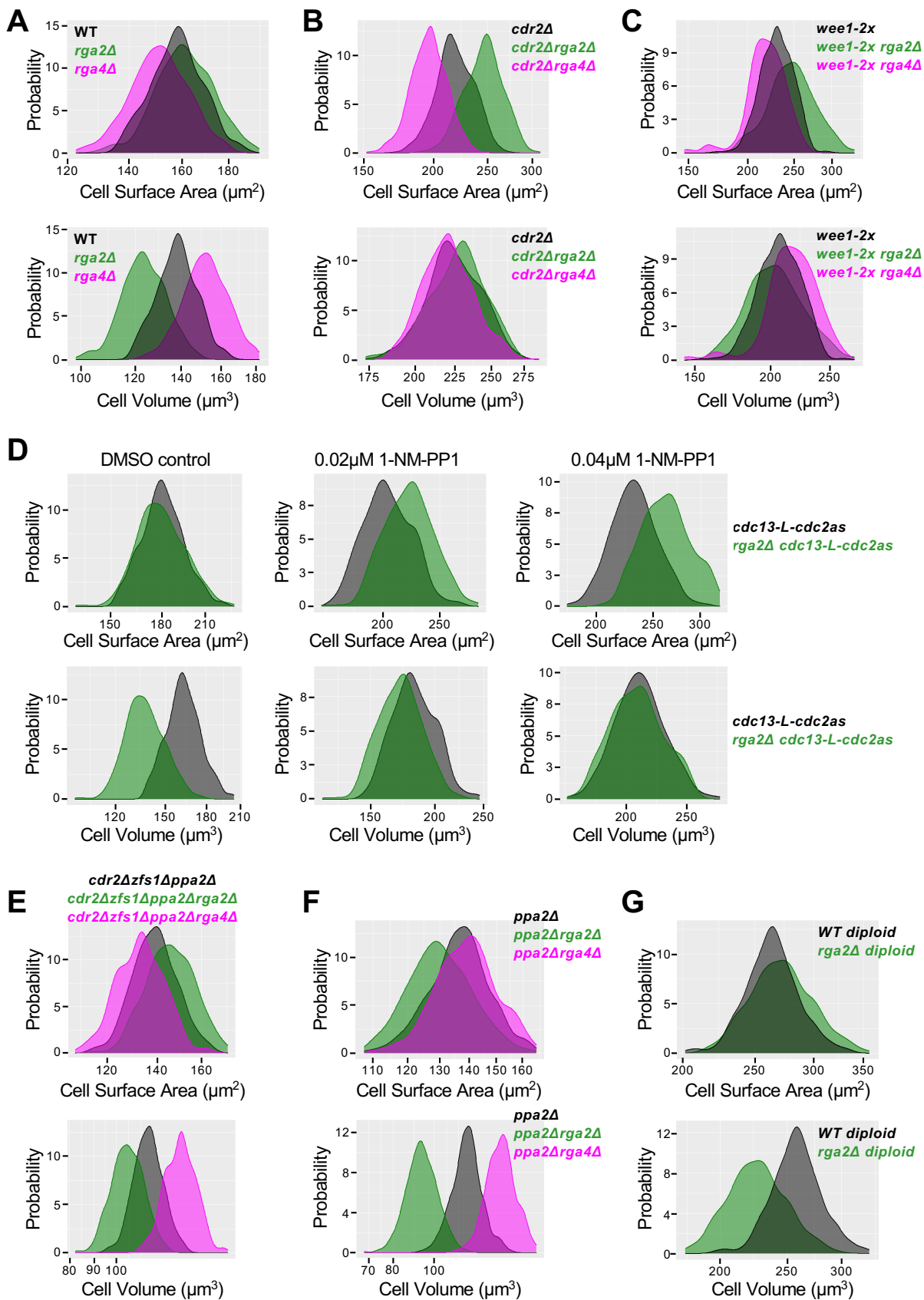
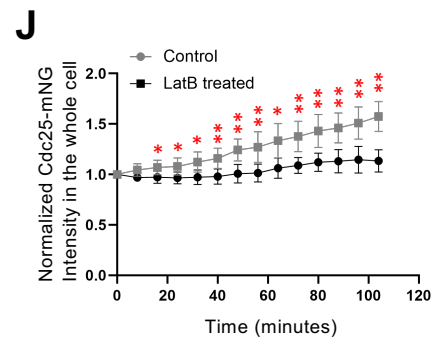
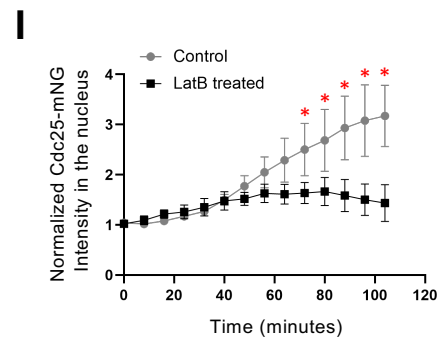
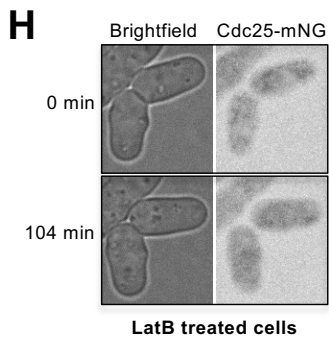
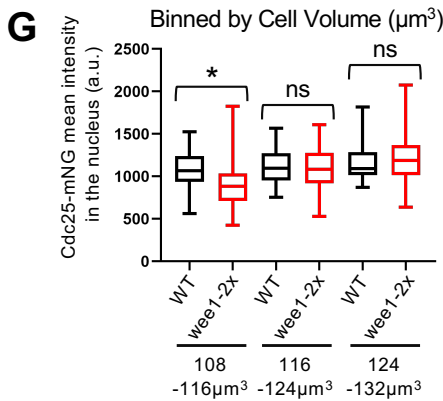
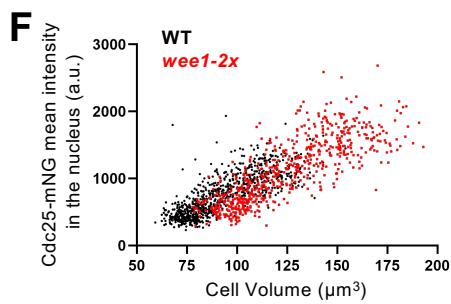
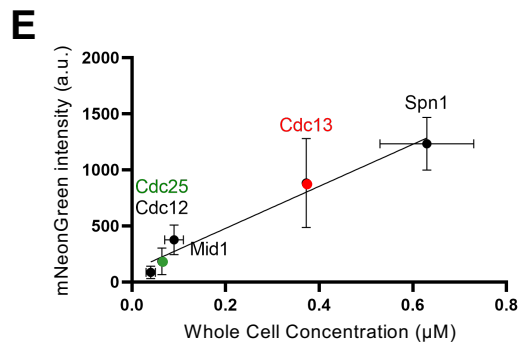
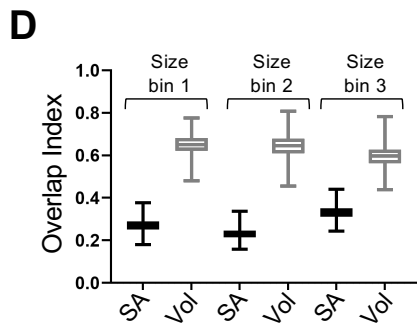
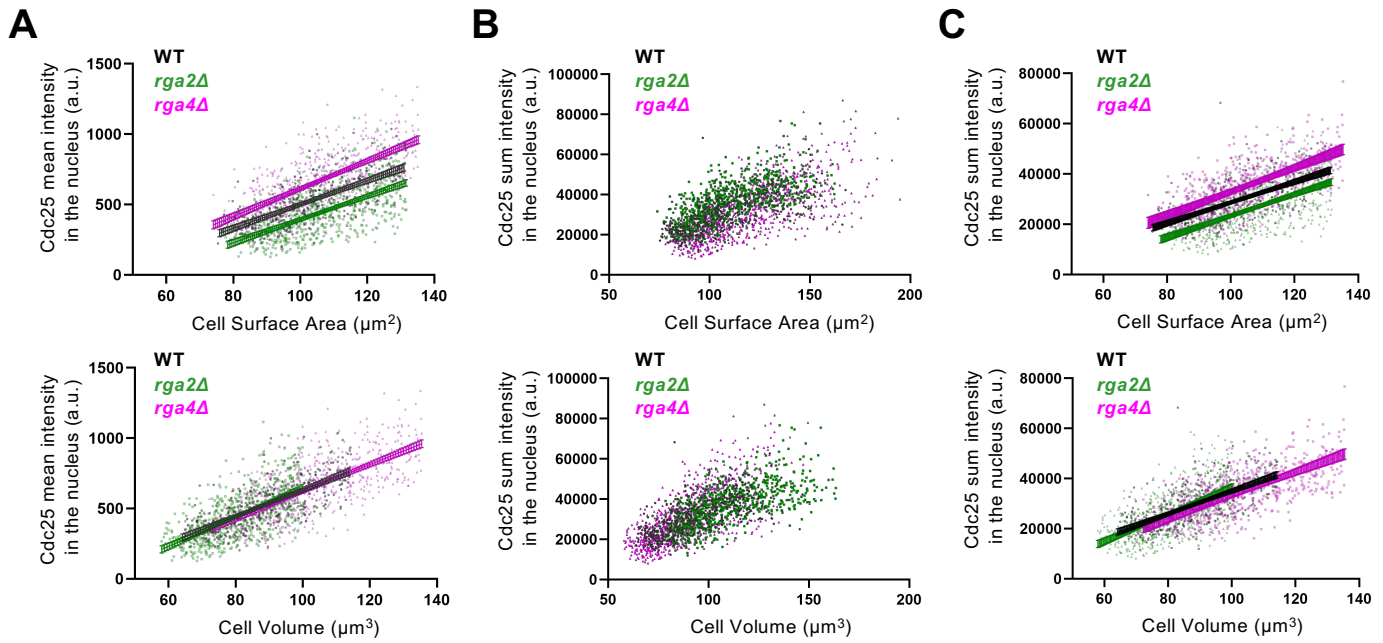


**Figure S1. Semi-automated image analysis pipeline to measure cell and nuclear size along with fluorescent protein intensities. Related to Figure 1, 4, 5, and STAR methods.** (A) Workflow for semi-automated image analysis. This example shows *cdc25-mNG BFP-NLS* cells imaged by spinning disk confocal microscopy. ImageJ is used to generate cell masks from brightfield images and nuclear masks from BFP-NLS images. MATLAB is used to segment cells and nuclei, assigning each nucleus to a cell. Our MATLAB code calculates cell/nuclear size (length, surface area, volume) as well as fluorescent intensities in the whole cell, nucleus, and cytoplasm. (B) This pipeline was validated using skinny (*rga2Δ*) and wide (*rga4Δ*) mutants to confirm that cells divide at a constant surface area, as opposed to volume. WT, n=480; *rga2Δ*, n=441; *rga4Δ*, n=760. (C) Overlap index analysis for the data in panel B. SA, surface area. Vol, volume. (D) Size measurements were verified by a rotation method (see STAR methods) that confirmed the robustness of our results. Graphs show WT, *rga2Δ*, and *rga4Δ* cell size at division plotted by cell surface area or volume. WT, n=480; *rga2Δ*, n=441; *rga4Δ*, n=760. (E) Overlap index analysis for the data in panel D. SA, surface area. Vol, volume. (F) Our pipeline confirms that *cdr2Δ* cells divide at a constant volume as opposed to surface area, as previously shown.<sup>20</sup> *cdr2Δ*, n=589; *cdr2Δrga2Δ*, n=733; *cdr2Δrga4Δ*, n=1021. (G) Overlap index analysis for data in panel D. (H) Analysis of *cdr2Δ* cell size at division using rotation method (See methods for details). *cdr2Δ*, n=589; *cdr2Δrga2Δ*, n=733; *cdr2Δrga4Δ*, n=1021. (I) Overlap index analysis for data in panel H. (J) The whole cell concentration ( $\mu\text{M}$ ) of Cdc25-mNG increases with cell size. Cells are binned by cell surface area (n>250 for each size bin). (K) The whole cell concentration ( $\mu\text{M}$ ) of Cdc13-mNG increases with cell size. Cells are binned by cell surface area. n>280 for each size bin. (L) Cell length at division ( $\mu\text{m}$ ) for the indicated strains and conditions. WT, n=268; *cdr2Δ*, n=590; *ppa2Δ*, n=294; *wee1-2x*, n=449; *cdc13-L-cdc2as*: DMSO n=686, 0.02 $\mu\text{M}$  1-NM-PP1 n=424, 0.04 $\mu\text{M}$  1-NM-PP1 n=470. All graphs show median as a line, quartiles, max, and min.



**Figure S2. Overlap index graphs. Related to Figure S1, 1, 2, and 3.** Graphs show probability of cell surface area or volume at division of indicated cell types and are a visual representation of the overlap index for the following experiments: (A) Dividing WT, *rga2Δ*, and *rga4Δ* cells in Figure S1B-C; (B) Dividing *cdr2Δ* cells in Figure S1D-F; (C) Dividing *wee1-2x* cells in Figure 1D-E; (D) dividing *cdc13-L-cdc2as* cells with indicated treatments in Figure 1G-H; (E) dividing *cdr2Δ zfs1Δ ppa2Δ* cells in Figure 2C-D; (F) dividing *ppa2Δ* cells in Figure 3B-C; (G) dividing diploid cells in Figure 3E-F.



**Figure S3. Additional analysis of Cdc25 nuclear accumulation. Related to Figure 4.** (A) The same plots of Cdc25-mNG nuclear intensity as Figure 4A, but with mitotic cells removed and linear regression lines for each cell type shown. (B) Cdc25-mNG sum intensity in the nucleus of WT, *rga2* $\Delta$ , and *rga4* $\Delta$  single cells plotted by cell surface area ( $\mu\text{m}^2$ ) or cell volume ( $\mu\text{m}^3$ ) (WT n=502, *rga2* $\Delta$  n=867, and *rga4* $\Delta$  n=684). Note that the same result is obtained by plotting sum intensity as by plotting mean intensity (See Figure 4A). (C) The same plots as Figure S3B but with mitotic cells removed and linear regression lines for each cell type shown. (D) Overlap index analysis for results in main Figure 4C, which show Cdc25-mNG nuclear intensity for cells binned by their cell surface area or volume. SA, surface area. Vol, volume. (E) Standard curve for calculating Cdc13 (Figure 5C and S1K) and Cdc25 (Figure 4D and S1J) concentrations ( $\mu\text{M}$ ). Error bars indicate SD. Linear regression used to interpolate experimental values. Fim1 and Arp2 were used to generate the standard curve but are not pictured here. Whole cell concentrations for standard proteins taken from Wu and Pollard (2005). (F) Cdc25-mNG mean intensity in the nucleus of WT and *wee1-2x* cells plotted by their cell volume (WT n=853; *wee1-2x* n=657). (G) WT and *wee1-2x* cells of the same volume have similar levels of Cdc25-mNG in the nucleus (n>110 per strain). Note that the same result is obtained when comparing WT and *cdr2* $\Delta$  cells (Figure 4E and 4F). (H) Representative time-lapse image of *cdc25-mNG* cells grown in the presence of 100 $\mu\text{M}$  Latrunculin B (LatB). Cdc25-mNG does not accumulate in the nucleus when growth is inhibited by addition of 100 $\mu\text{M}$  LatB, an actin inhibitor. (I) Mean normalized nuclear Cdc25-mNG intensity or (J) mean normalized Cdc25-mNG intensity in the whole cell over time in individual cells treated with or without 100 $\mu\text{M}$  LatB. n=10 cells per condition. Error bars indicate SD. Asterisks indicate significant difference in fluorescent intensity (p>0.05) at given time point.

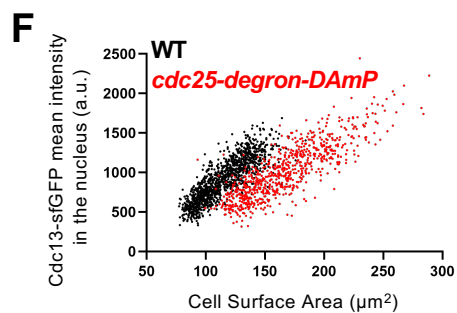
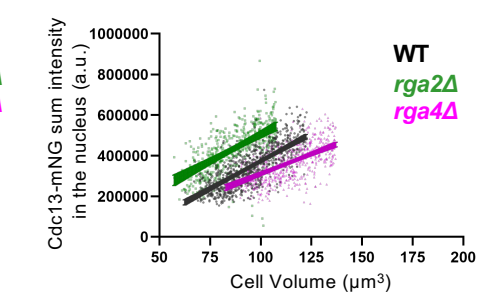
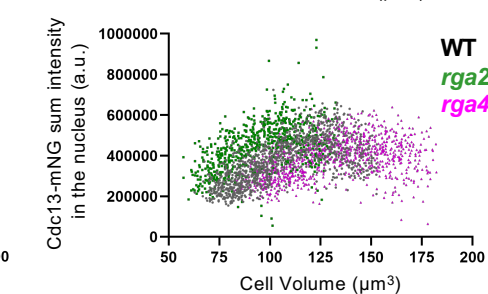
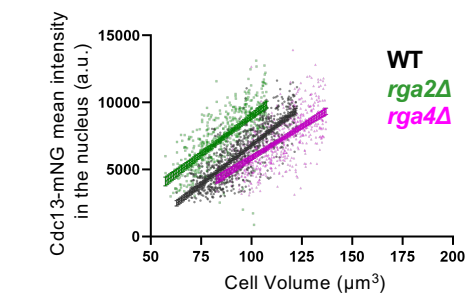
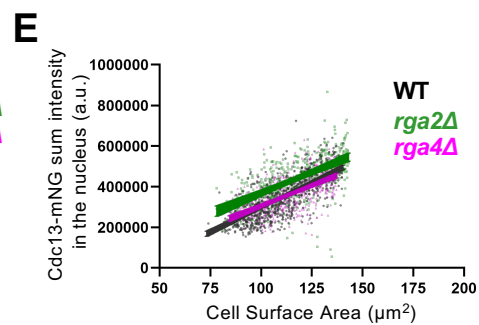
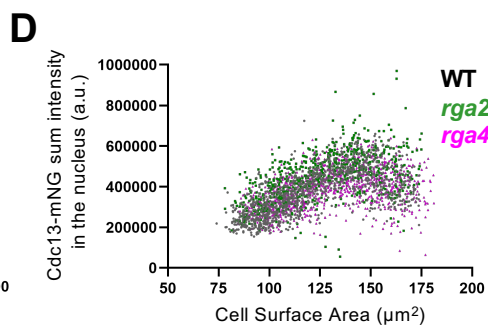
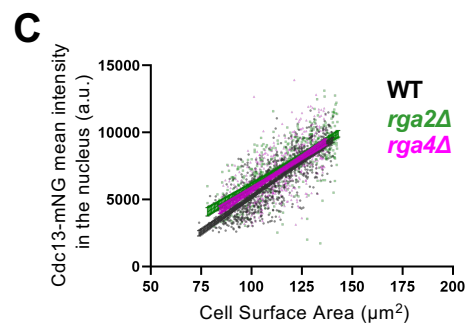
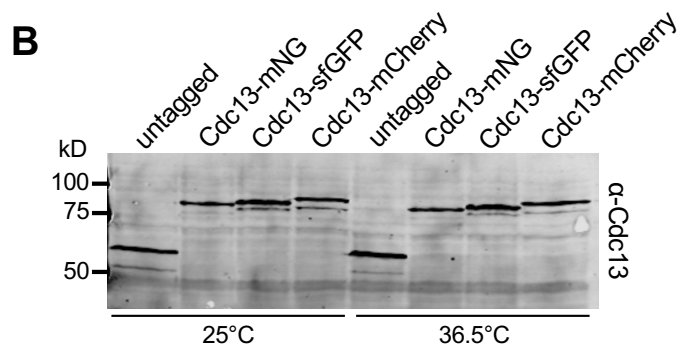
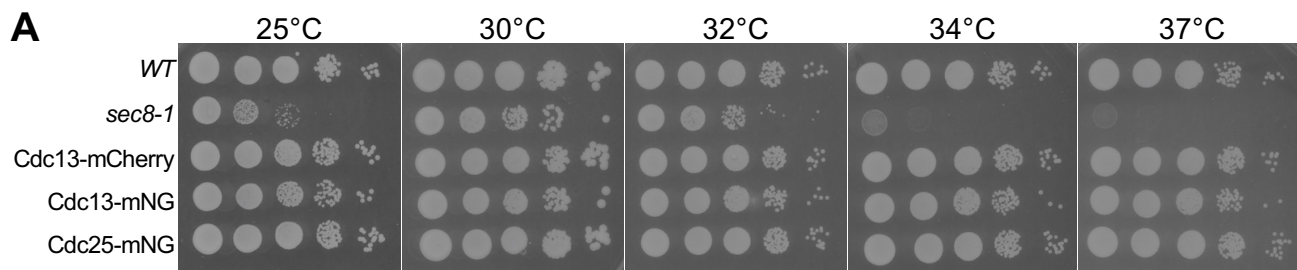


**Figure S4. Additional analysis of Cdc13. Related to Figure 5.** (A) The indicated strains were spotted with 10 $\times$  serial dilutions onto YE4S plates. Plates were incubated for 2-4 days prior to imaging. Yeast cells expressing tagged Cdc13 or Cdc25 do not exhibit growth defects. (B) Western blot of whole cell extracts from the indicated strains. Cells were grown at 25 $^{\circ}$ C or 36.5 $^{\circ}$ C for 5 hours before harvesting. Anti-Cdc13 antibody was used to test if fusion proteins were cleaved under experimental conditions used in this study. No untagged or cleaved Cdc13 protein was detected in cells expressing Cdc13-mNG, Cdc13-sfGFP, or Cdc13-mCherry. (C) The same plots of Cdc13-mNG nuclear accumulation as Figure 5A, but with mitotic cells removed and linear regression lines for each cell type shown. (D) Cdc13-mNG sum intensity in the nucleus of WT, *rga2* $\Delta$ , and *rga4* $\Delta$  single cells plotted by cell surface area ( $\mu\text{m}^2$ ) or cell volume ( $\mu\text{m}^3$ ) (WT n=1,166, *rga2* $\Delta$  n=687, and *rga4* $\Delta$  n=1,019). Note that the same result is obtained by plotting sum intensity as by plotting mean intensity (See Figure 5A). (E) The same plots as Figure S4D but with mitotic cells removed and linear regression lines for each cell type shown. (F) Cdc13-sfGFPint mean intensity in the nucleus of WT and *cdc25-degtron-DAmP* cells plotted by their surface area with mitotic cells removed (WT n=1,261; *cdc25-degtron-DAmP* n=804). Note that the same result is obtained when comparing WT and *cdr2* $\Delta$  cells (Figure 5D and 5E).

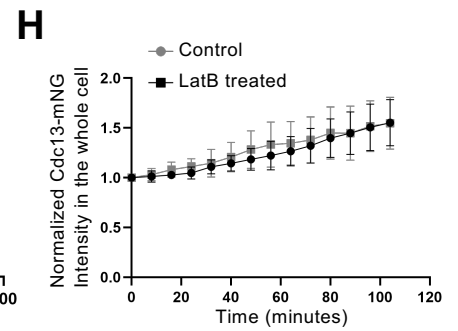
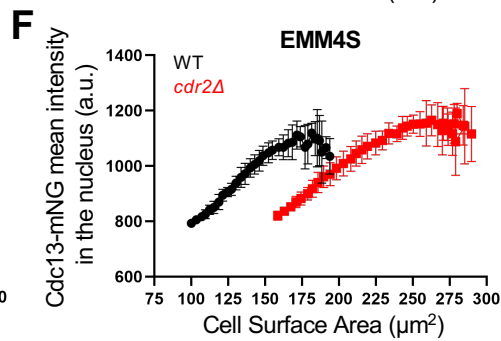
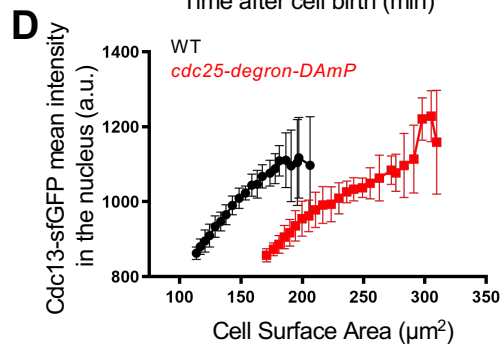
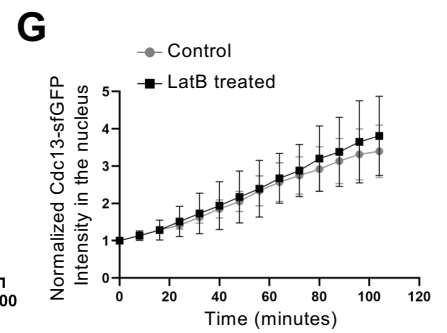
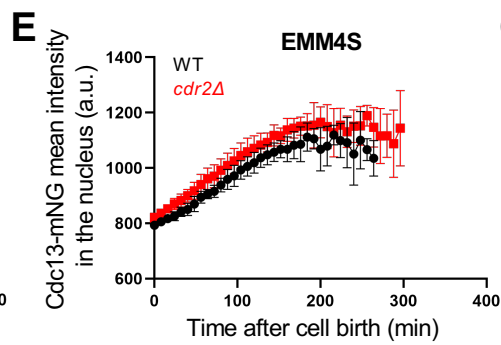
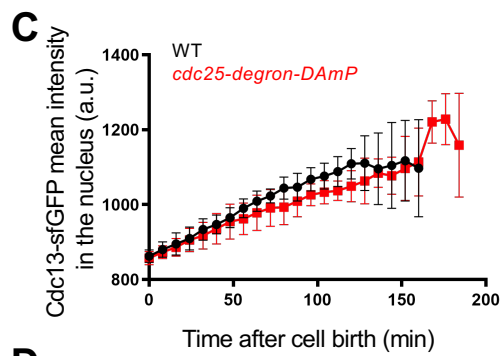
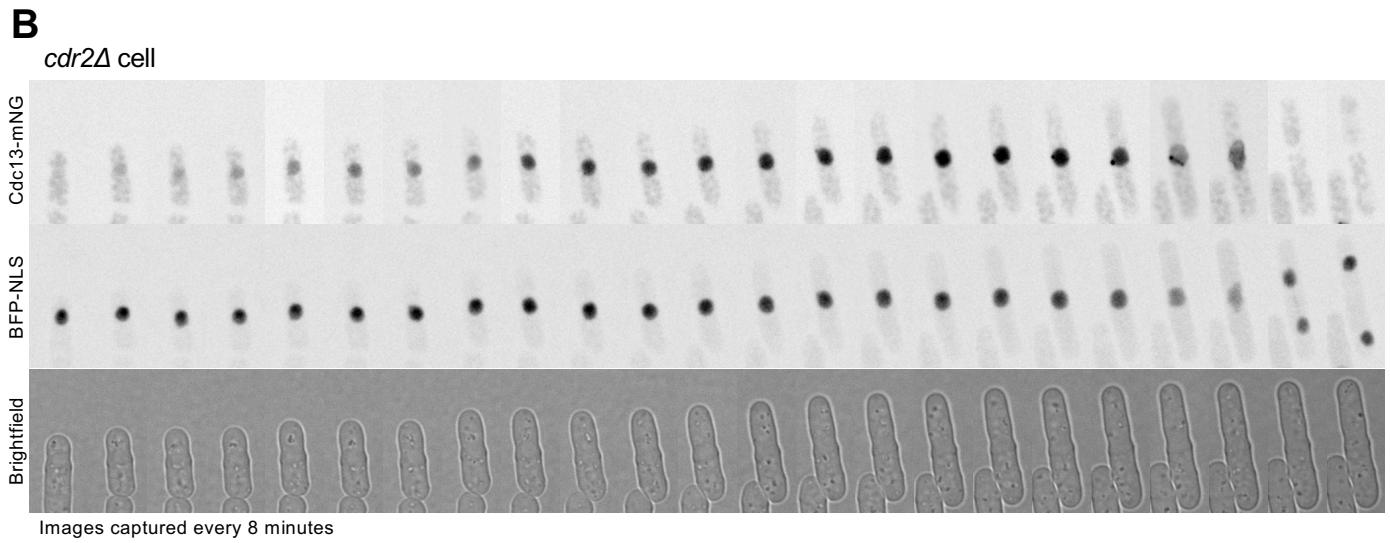
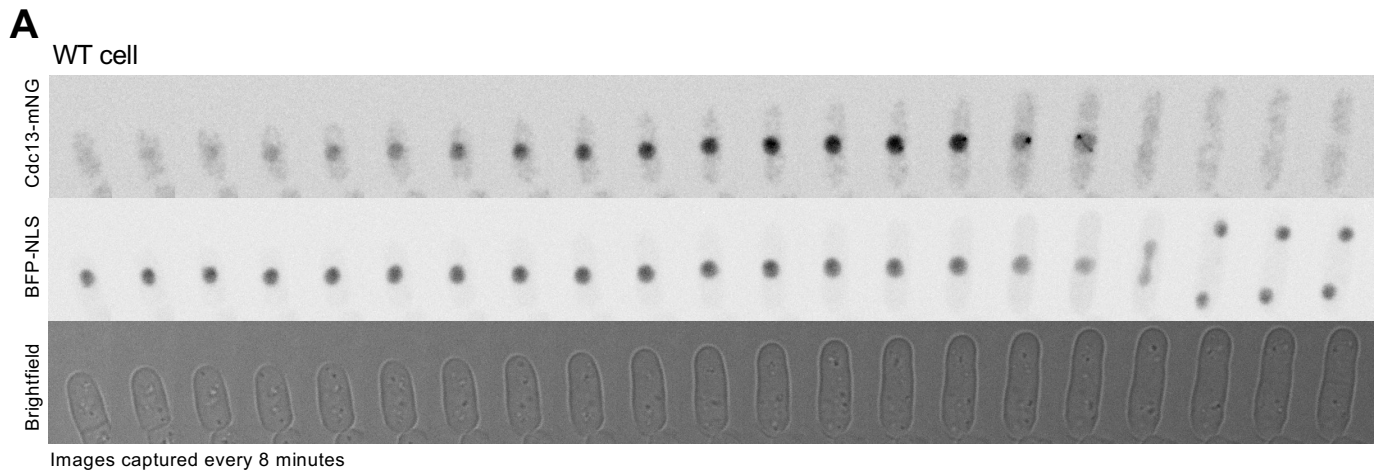




**Figure S5. Time-lapse imaging of Cdc13-mNG in wild type and *cdr2* $\Delta$  cells. Related to Figure 5.** Time-lapse images of Cdc13-mNG, BFP-NLS, and cell dimensions by brightfield in WT (A) and *cdr2* $\Delta$  cells (B). Images captured every 8 minutes. Images are inverted maximum projection images, except brightfield images are single middle z sections. (C-D) Average Cdc13-sfGFP<sup>int</sup> mean intensity in the nucleus of single cells from time-lapse imaging WT or *cdc25-degron-DAmP* cells. n=10 cells per strain. Error bars indicate SD. Cdc13-sfGFP<sup>int</sup> nuclear concentration was plotted either by time since cell birth (panel C) or by cell surface area (panel D). Note that the same result is obtained when comparing WT and *cdr2* $\Delta$  cells (Figure 5F and 5G). (E-F) Average Cdc13-mNG mean intensity in the nucleus of single cells from time-lapse imaging WT or *cdr2* $\Delta$  cells grown in minimal EMM4S media. n=10 cells per strain. Error bars indicate SD. Cdc13-mNG nuclear concentration was plotted either by time since cell birth (panel E) or by cell surface area (panel F). Note that the same result is obtained when comparing WT and *cdr2* $\Delta$  cells (or *cdc25-degron-DAmP*) cells in YE4S media by time-lapse imaging (Figure 5F, 5G, S5C, and S5D). (G) Mean normalized nuclear Cdc13-sfGFP<sup>int</sup> intensity over time in individual cells treated with or without 100 $\mu$ M LatB. n=10 cells per experiment. Error bars indicate SD. Note that the same result is obtained when using Cdc13-mNG containing cells (Figure 5I). (H) Mean normalized Cdc13-mNG intensity in the whole cell over time in individual cells treated with or without 100 $\mu$ M LatB. n=10 cells per experiment (Same cells as Figure 5I). Error bars indicate SD.

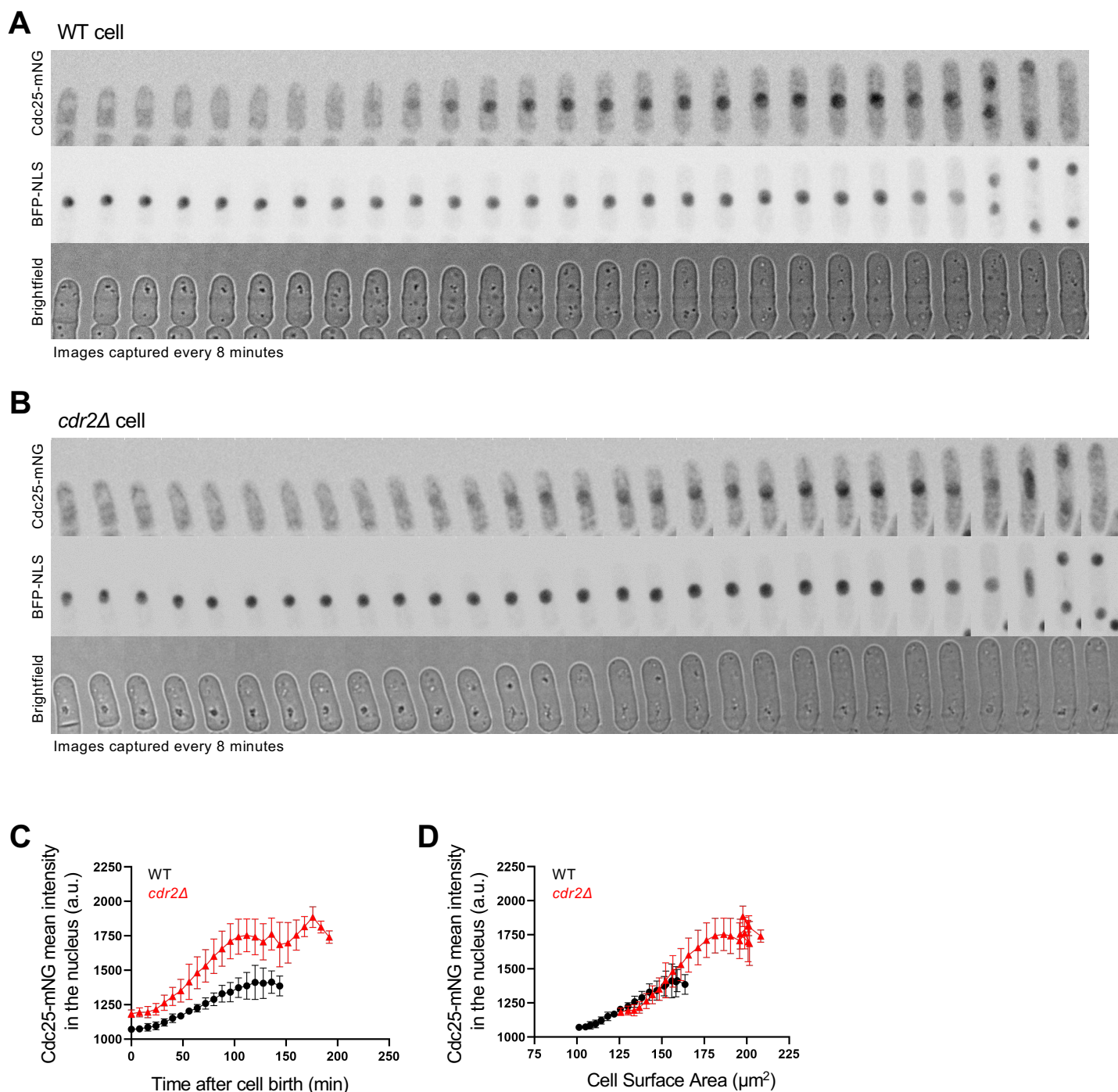


**Figure S6. Time-lapse imaging of Cdc25-mNG in wild type and *cdr2Δ* cells. Related to Figure 4.** Time-lapse images of Cdc25-mNG, BFP-NLS, and cell dimensions by brightfield in WT (A) and *cdr2Δ* cells (B). Images captured every 8 minutes. Images are inverted maximum projection images, except brightfield images are single middle z sections. (C-D) Average Cdc25-mNG mean intensity in the nucleus of single cells from time-lapse imaging WT or *cdr2Δ* cells.  $n=10$  cells per strain. Error bars indicate SD. Cdc25-mNG nuclear concentration was plotted either by time since cell birth (panel C) or by cell surface area (panel D). Note that Cdc25 nuclear accumulation scaling with cell size is also shown by static image analysis (Figure 4E, 4F, S3F, and S3G).

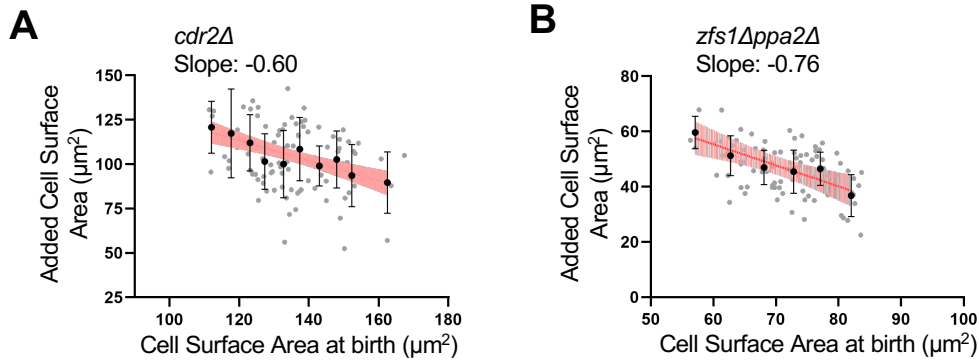


**Figure S7. Additional cell size homeostasis analysis. Related to Figure 6.** (A-B) Size homeostasis plots of *cdr2Δ* (A), and *zfs1Δ ppa2Δ* (B) cells. The cell surface area at birth and added surface area for individual cells was determined from timelapse imaging. Plots show data from individual cells (grey circles) and mean cell surface area at birth and added surface area for 5 $\mu\text{m}^2$  cell surface area size bins (black circles). Black bars indicate SD. Slope of linear regression line (red) displayed below cell type for each graph. Vertical light red lines along linear regression line indicate 95% confidence of the best-fit line. *cdr2Δ*, n=101; *zfs1Δ ppa2Δ*, n=101. Size homeostasis experiments were repeated at least 2 times and representative graphs from one experiment are shown.

	Yeast strain genotype	Mean Width ( $\mu\text{m}$ ) $\pm$ SD	Mean Length ( $\mu\text{m}$ ) $\pm$ SD
	<i>WT</i>	3.60 $\pm$ 0.2	14.03 $\pm$ 0.9
	<i>rga2</i> $\Delta$	3.10 $\pm$ 0.2	16.33 $\pm$ 1.2
	<i>rga4</i> $\Delta$	4.04 $\pm$ 0.1	12.00 $\pm$ 1.0
	<i>cdr2</i> $\Delta$	3.69 $\pm$ 0.2	17.00 $\pm$ 1.3
	<i>cdr2</i> $\Delta$ <i>rga2</i> $\Delta$	3.23 $\pm$ 0.2	20.84 $\pm$ 1.7
	<i>cdr2</i> $\Delta$ <i>rga4</i> $\Delta$	4.20 $\pm$ 0.3	13.74 $\pm$ 1.0
	<i>wee1-2x</i>	3.54 $\pm$ 0.2	20.00 $\pm$ 1.5
	<i>rga2</i> $\Delta$ <i>wee1-2x</i>	3.18 $\pm$ 0.1	24.00 $\pm$ 2.7
	<i>rga4</i> $\Delta$ <i>wee1-2x</i>	4.14 $\pm$ 0.3	17.29 $\pm$ 1.6
DMSO	<i>cdc13-L-cdc2as</i>	3.72 $\pm$ 0.2	15.57 $\pm$ 1.2
DMSO	<i>rga2</i> $\Delta$ <i>cdc13-L-cdc2as</i>	3.12 $\pm$ 0.2	18.31 $\pm$ 1.6
0.02 $\mu\text{M}$ PP1	<i>cdc13-L-cdc2as</i>	3.70 $\pm$ 0.1	17.83 $\pm$ 1.7
0.02 $\mu\text{M}$ PP1	<i>rga2</i> $\Delta$ <i>cdc13-L-cdc2as</i>	3.19 $\pm$ 0.2	22.42 $\pm$ 2.2
0.04 $\mu\text{M}$ PP1	<i>cdc13-L-cdc2as</i>	3.76 $\pm$ 0.2	20.09 $\pm$ 1.8
0.04 $\mu\text{M}$ PP1	<i>rga2</i> $\Delta$ <i>cdc13-L-cdc2as</i>	3.20 $\pm$ 0.2	26.01 $\pm$ 2.5
	<i>cdr2</i> $\Delta$ <i>ppa2</i> $\Delta$ <i>zfs1</i> $\Delta$	3.50 $\pm$ 0.2	13.00 $\pm$ 0.9
	<i>cdr2</i> $\Delta$ <i>ppa2</i> $\Delta$ <i>zfs1</i> $\Delta$ <i>rga2</i> $\Delta$	3.0 $\pm$ 0.2	16.00 $\pm$ 1.2
	<i>cdr2</i> $\Delta$ <i>ppa2</i> $\Delta$ <i>zfs1</i> $\Delta$ <i>rga4</i> $\Delta$	4.22 $\pm$ 0.2	10.03 $\pm$ 0.8
	<i>ppa2</i> $\Delta$	3.78 $\pm$ 0.2	12.14 $\pm$ 1.0
	<i>ppa2</i> $\Delta$ <i>rga2</i> $\Delta$	3.12 $\pm$ 0.2	14.00 $\pm$ 1.1
	<i>ppa2</i> $\Delta$ <i>rga4</i> $\Delta$	4.42 $\pm$ 0.2	10.43 $\pm$ 0.8
	<i>WT diploid</i>	3.94 $\pm$ 0.2	21.18 $\pm$ 1.7
	<i>rga2</i> $\Delta$ <i>diploid</i>	3.38 $\pm$ 0.1	25.61 $\pm$ 2.5
interphase	<i>cdc25-mNG</i>	3.59 $\pm$ 1.8	10.00 $\pm$ 1.7
interphase	<i>rga2</i> $\Delta$ <i>cdc25-mNG</i>	3.15 $\pm$ 1.6	12.04 $\pm$ 2.4
interphase	<i>rga4</i> $\Delta$ <i>cdc25-mNG</i>	4.13 $\pm$ 2.1	8.55 $\pm$ 1.5
interphase	<i>cdc13-mNG</i>	3.60 $\pm$ 0.13	10.77 $\pm$ 2.2
interphase	<i>rga2</i> $\Delta$ <i>cdc13-mNG</i>	3.10 $\pm$ 0.2	12.97 $\pm$ 2.4
interphase	<i>rga4</i> $\Delta$ <i>cdc13-mNG</i>	4.15 $\pm$ 0.2	9.85 $\pm$ 1.7

**Table S1. Cell length and width of yeast strains. Related to STAR methods.** Cell widths were measured by hand from cell masks as described in the methods. Cell lengths were measured from cell masks by MATLAB. All length and width values are from dividing cells except where noted.

Name	“Mean Radius of Cell Population”	“Rotation”
Description	Using average radius of cell population determined by manual measurements of individual cells	Rotation around the symmetry axis of each cell
Cell Radius	R	Function $R(x)^a$
Cell Length	L	L
Cell Surface Area	$2\pi RL$	$2\pi \int_0^L R(x) \sqrt{1 + R'(x)^2} dx$
Cell Volume	$\pi R^2 L - 2/3\pi R^3$	$\pi \int_0^L R^2(x) dx$

**Table S2. Calculation of cell surface area or volume. Related to STAR methods.** Description of equations used to measure cell surface area and volume of fission yeast cells.  $R(x)$  is defined as the shortest distance from the cell border to the symmetry axis,  $R(x)$ ,  $0 \leq x \leq L$

Nuclei minor axis	$mj$
Nuclei major axis	$mn$
Nuclei volume	$1/6\pi * mj * mn^2$

**Table S3. Calculation of nuclear size. Related to STAR methods.**

	N/C ratio, mean $\pm$ SD
WT, n=63	0.072 $\pm$ 0.01
<i>rga2</i> $\Delta$ , n=86	0.075 $\pm$ 0.01
<i>rga4</i> $\Delta$ , n=136	0.072 $\pm$ 0.01

**Table S4. Nuclear to cytoplasmic (N/C) volume ratios. Related to STAR methods.**